

1 Supplementary Information for “*Coupled Seasonal Data Assimilation of Sea*
2 *Ice, Ocean, and Atmospheric Dynamics over the Last Millennium*”

3 Zilu Meng^a, Gregory J. Hakim^a, Eric J. Steig^{b,a}

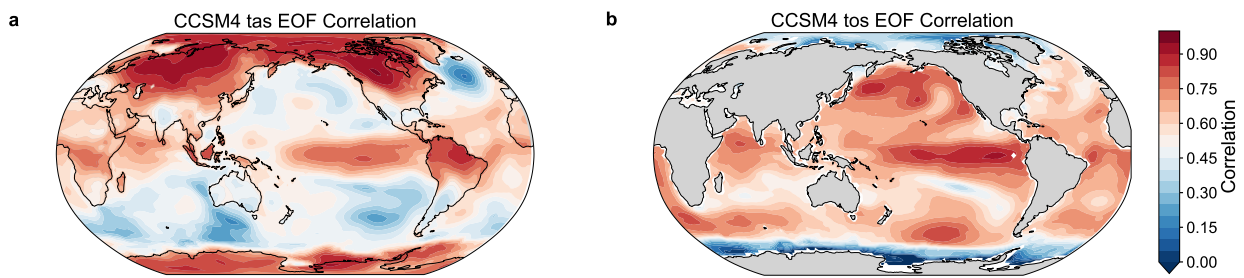
4 ^a*Department of Atmospheric and Climate Science, University of Washington, Seattle, Washington*

5 ^b*Department of Earth and Space Sciences, University of Washington, Seattle, Washington*

6 Corresponding author: Zilu Meng, zilumeng@uw.edu

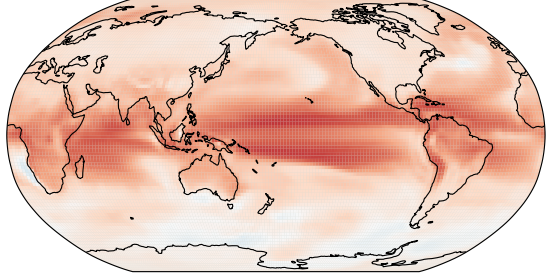
⁷ **Contents**

⁸ 1. SI Figure S1-S18.

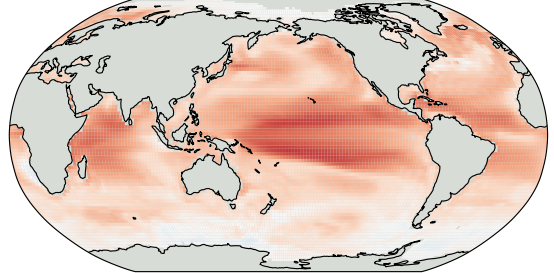


9 FIG. S1. Correlation between the EOF-truncated space (first 15 modes) and the original CCSM4 LM fields for
10 surface temperature (**a**, TAS) and sea surface temperature (**b**, TOS).

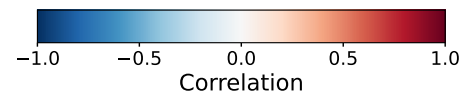
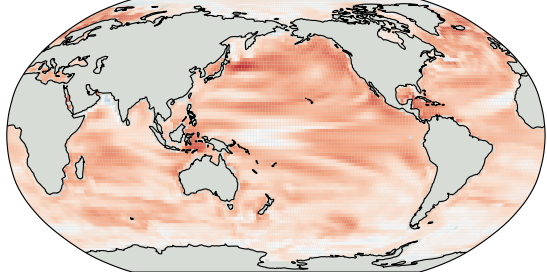
a. TAS; lead = 12 month; corr = 0.23



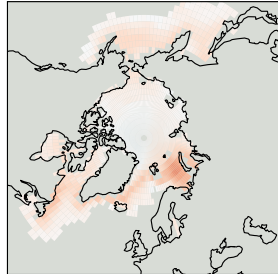
b. TOS; lead = 12 month; corr = 0.24



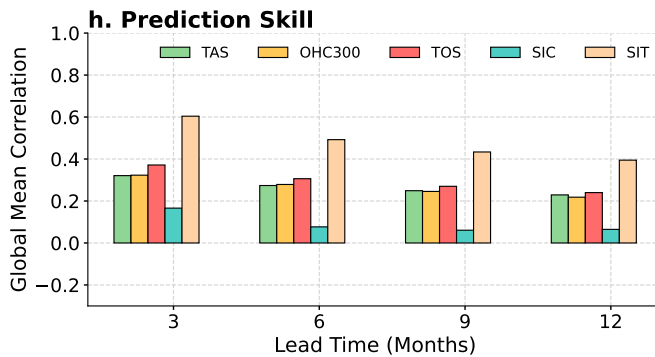
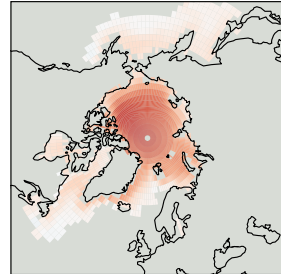
c. OHC300; lead = 12 month; corr = 0.22



d. SIC; lead = 12 month; corr = 0.06

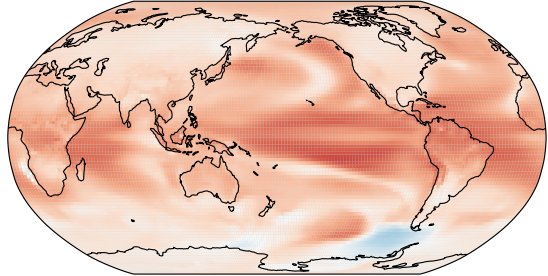


e. SIT; lead = 12 month; corr = 0.39

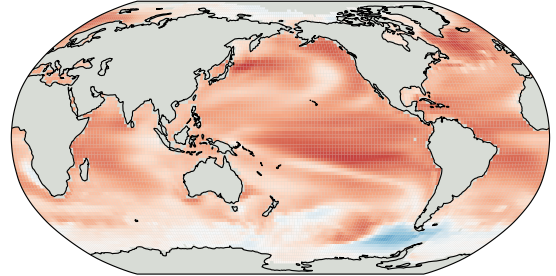


11 FIG. S2. Forecast skill of the Linear Inverse Model (LIM) trained on CCSM4 tested on MPI-ESM-R.
12 a-e. LIM correlation skill out-of-sample test on MPI-ESM-R at 12-month lead on TAS (a), TOS (b), OHC300
13 (c), SIC(d) and SIT (e). h. The global-mean forecast skill of different variables at lead time from 3 months to 12
14 months.

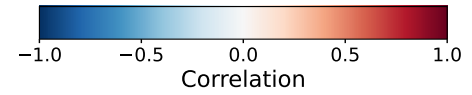
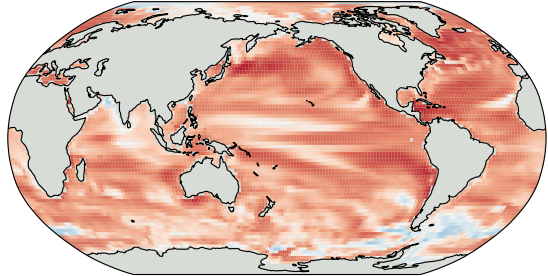
a. TAS; lead = 12 month; corr = 0.26



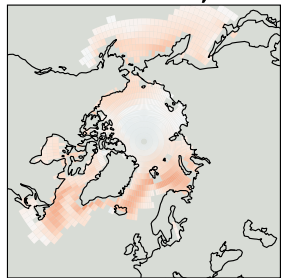
b. TOS; lead = 12 month; corr = 0.27



c. OHC300; lead = 12 month; corr = 0.35



d. SIC; lead = 12 month; corr = 0.08



e. SIT; lead = 12 month; corr = 0.43

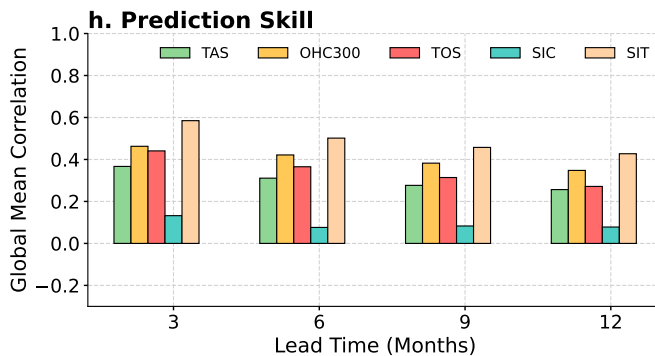
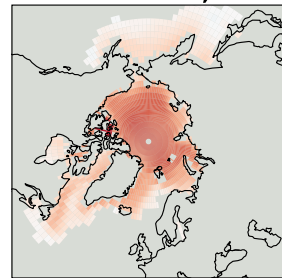


FIG. S3. As in Figure S2, but for the LIM trained on MPI-ESM-R and tested on CCSM4.

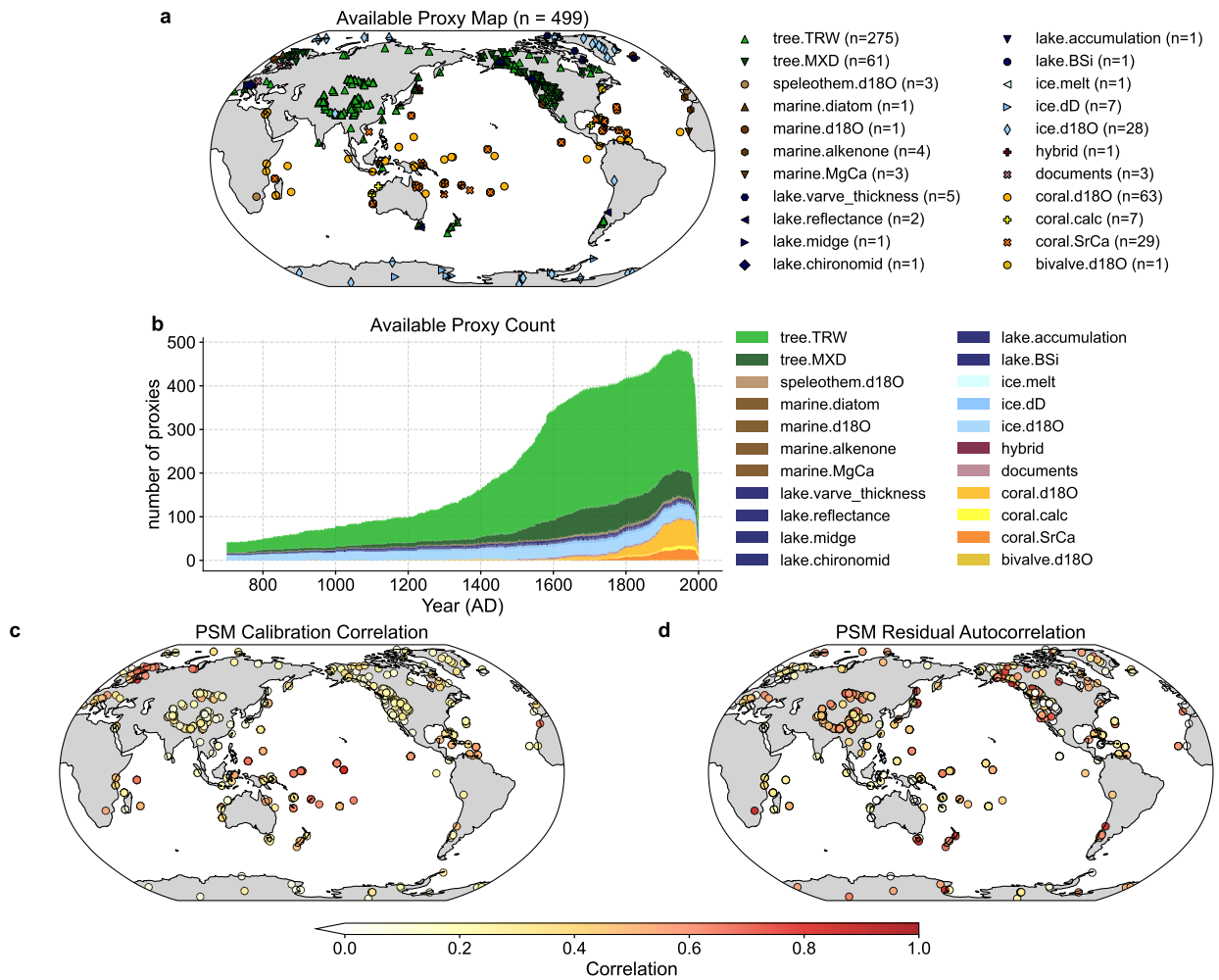


FIG. S4. As in Figure 1, but for PSMs based on expert-seasonality.

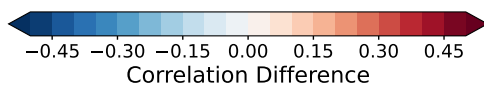
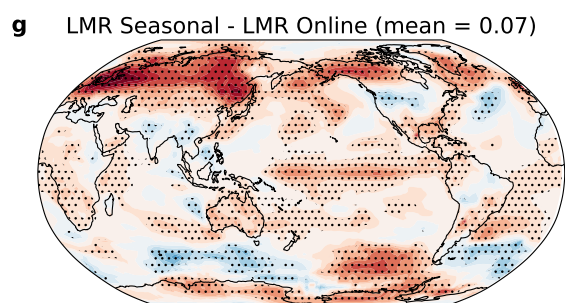
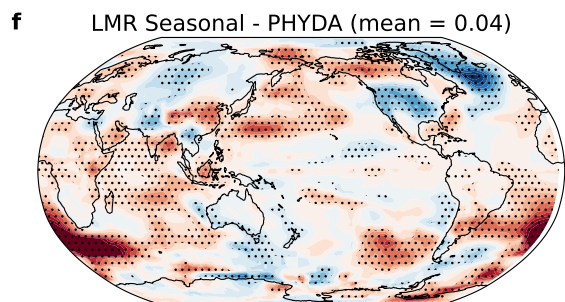
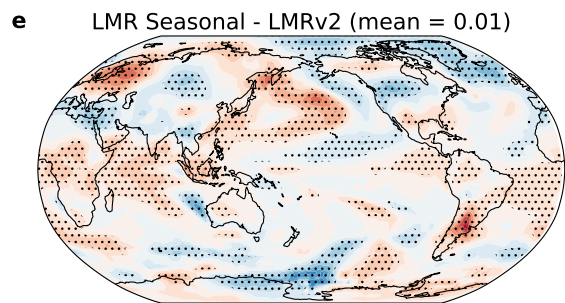
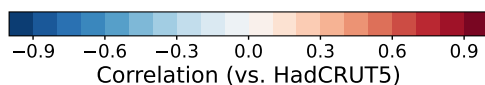
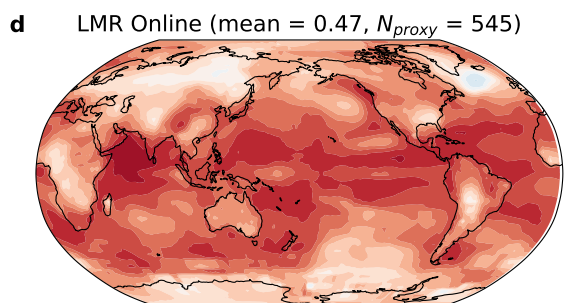
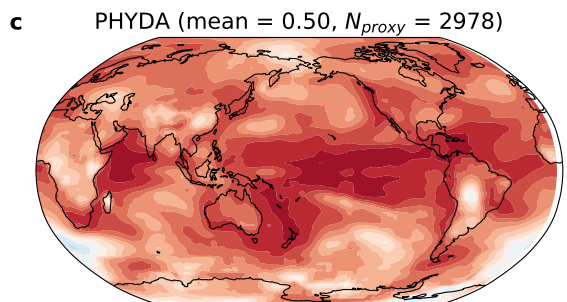
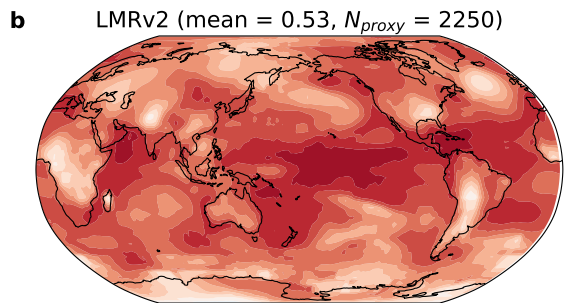
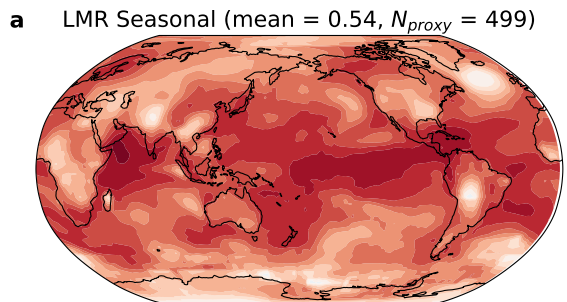


FIG. S5. As in Figure 3, but for the expert-seasonality based PSM.

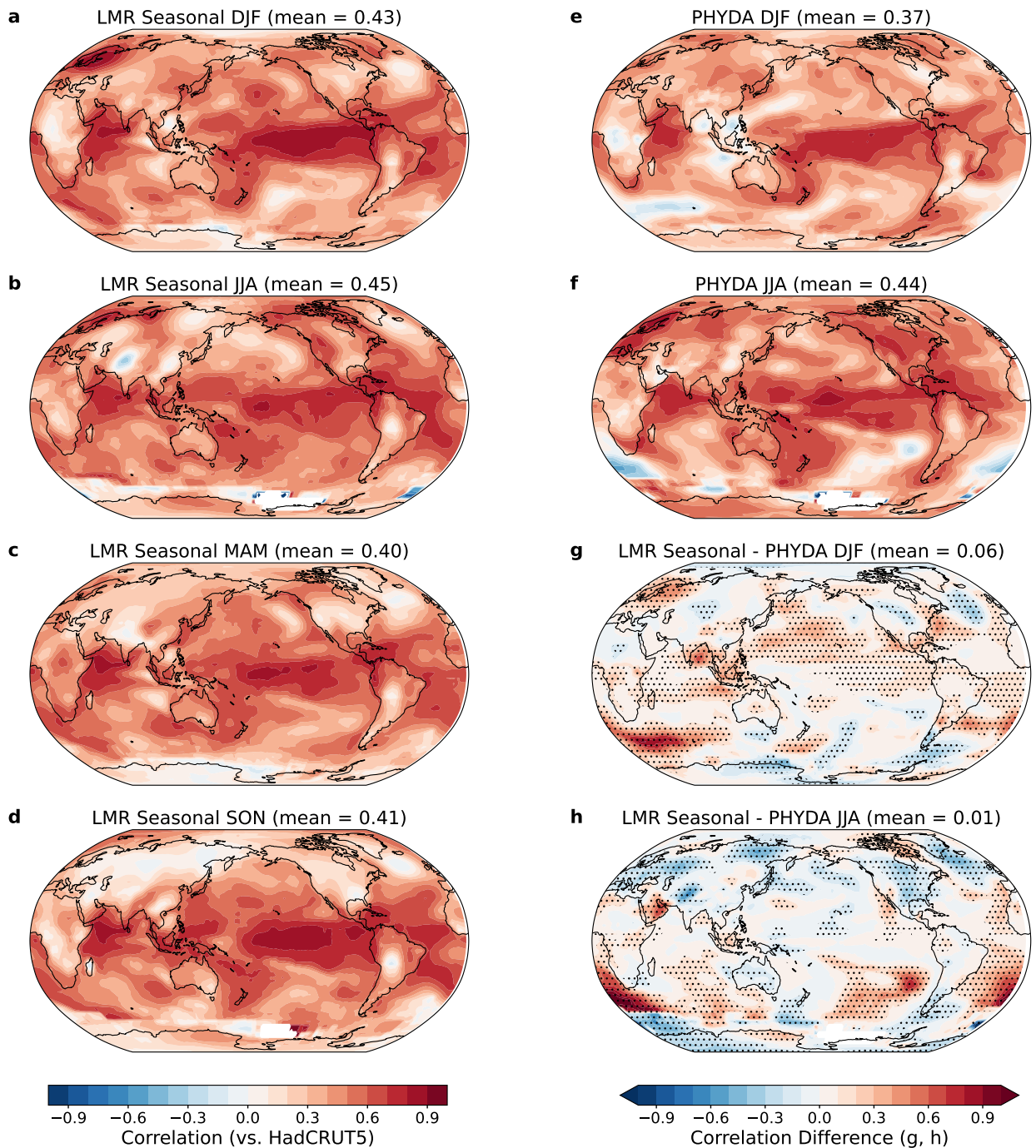


FIG. S6. As in Figure 4, but for the expert-seasonality based PSM.

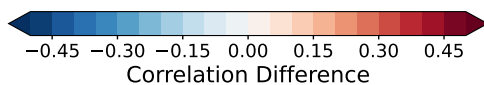
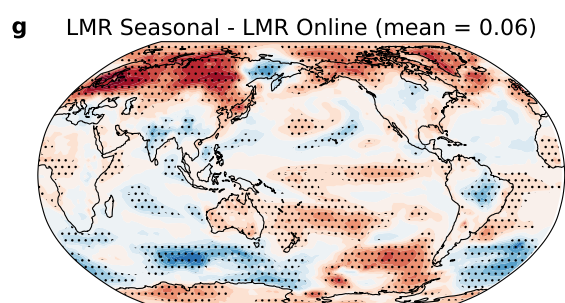
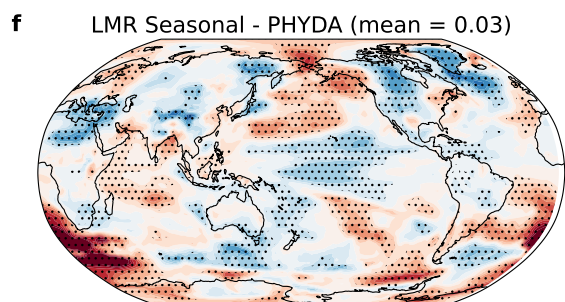
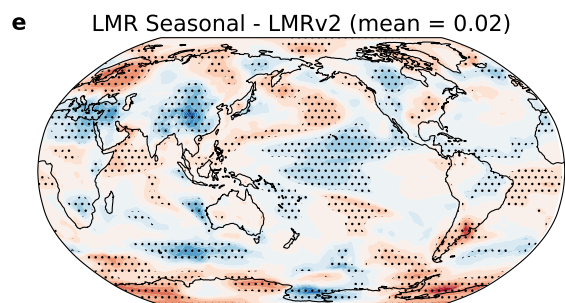
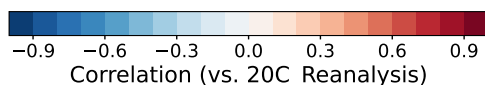
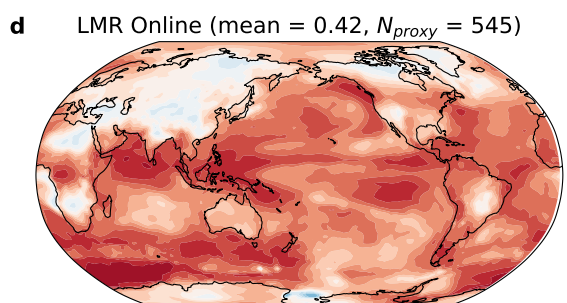
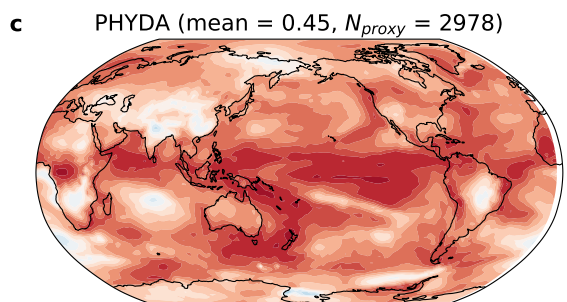
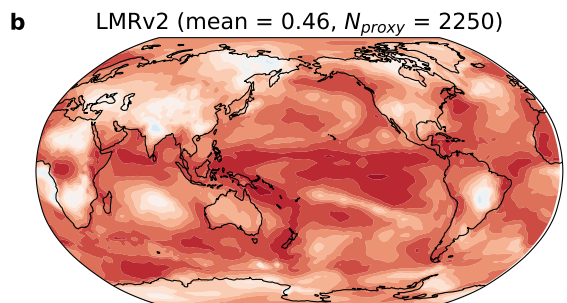
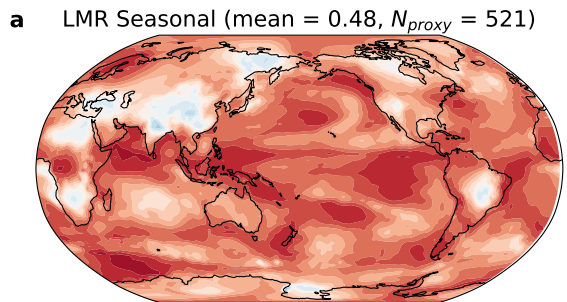


FIG. S7. As in Figure 3, but for the correlation between reconstructions and ERA-20C Reanalysis.

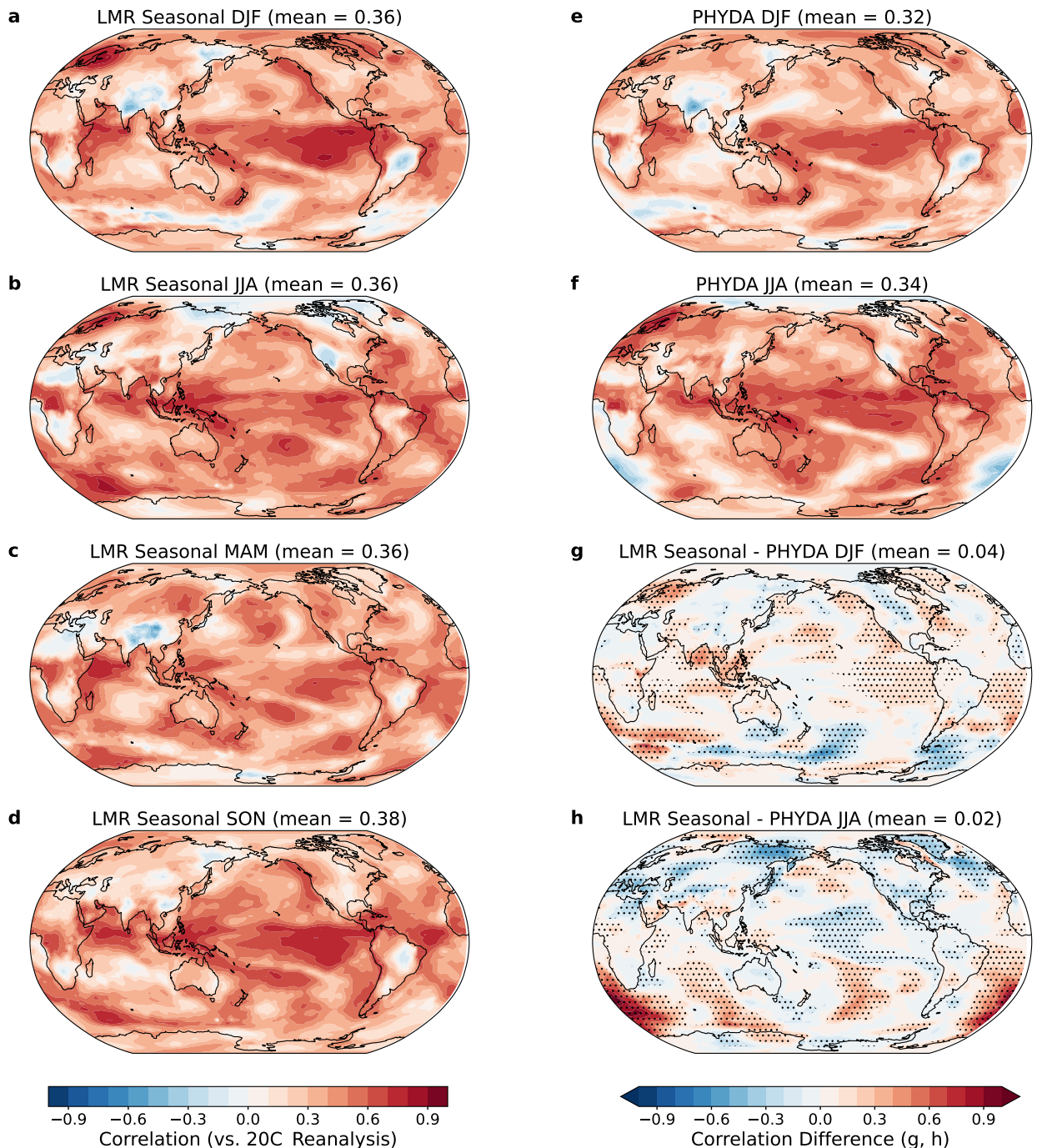
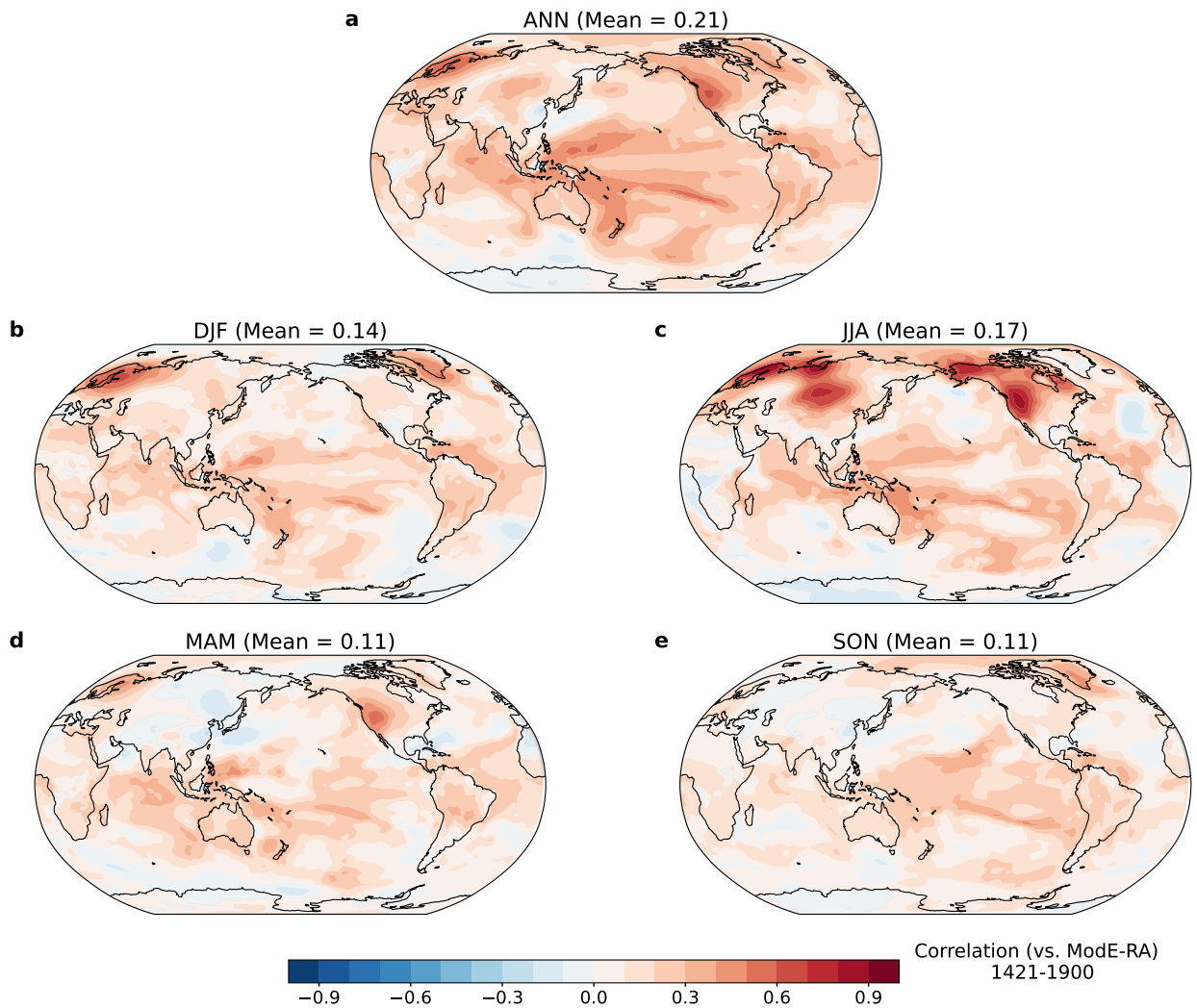


FIG. S8. As in Figure 4, but for the correlation between reconstructions and ERA-20C Reanalysis.



15 FIG. S9. Correlation between LMR Seasonal surface temperature and ModE-RA (Valler et al. 2024) surface
 16 temperature over the period 1421–1900 for the annual mean (a), DJF (b), JJA (c), MAM (d), and SON (e).
 17 Global-mean correlations are indicated in the titles.

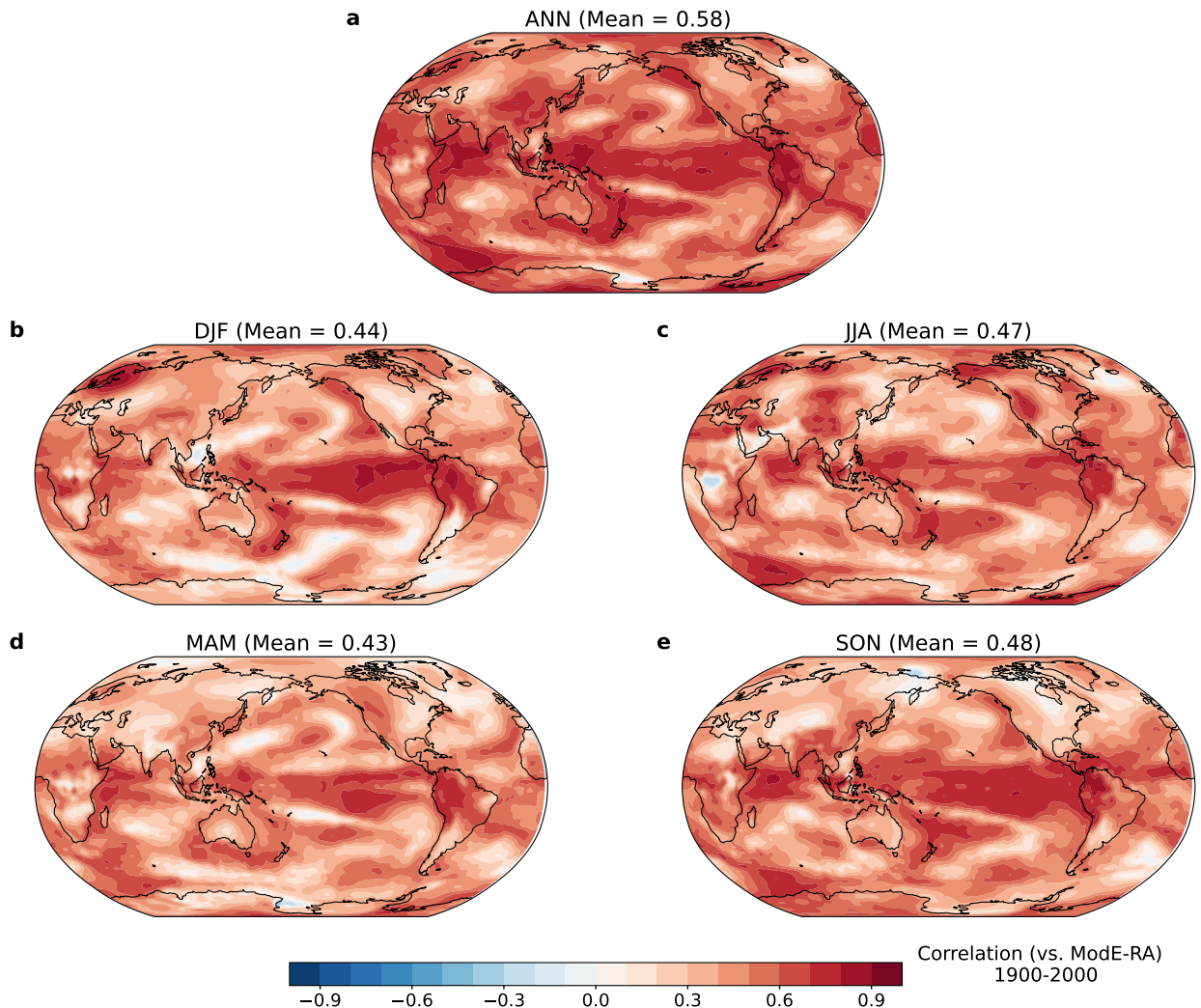
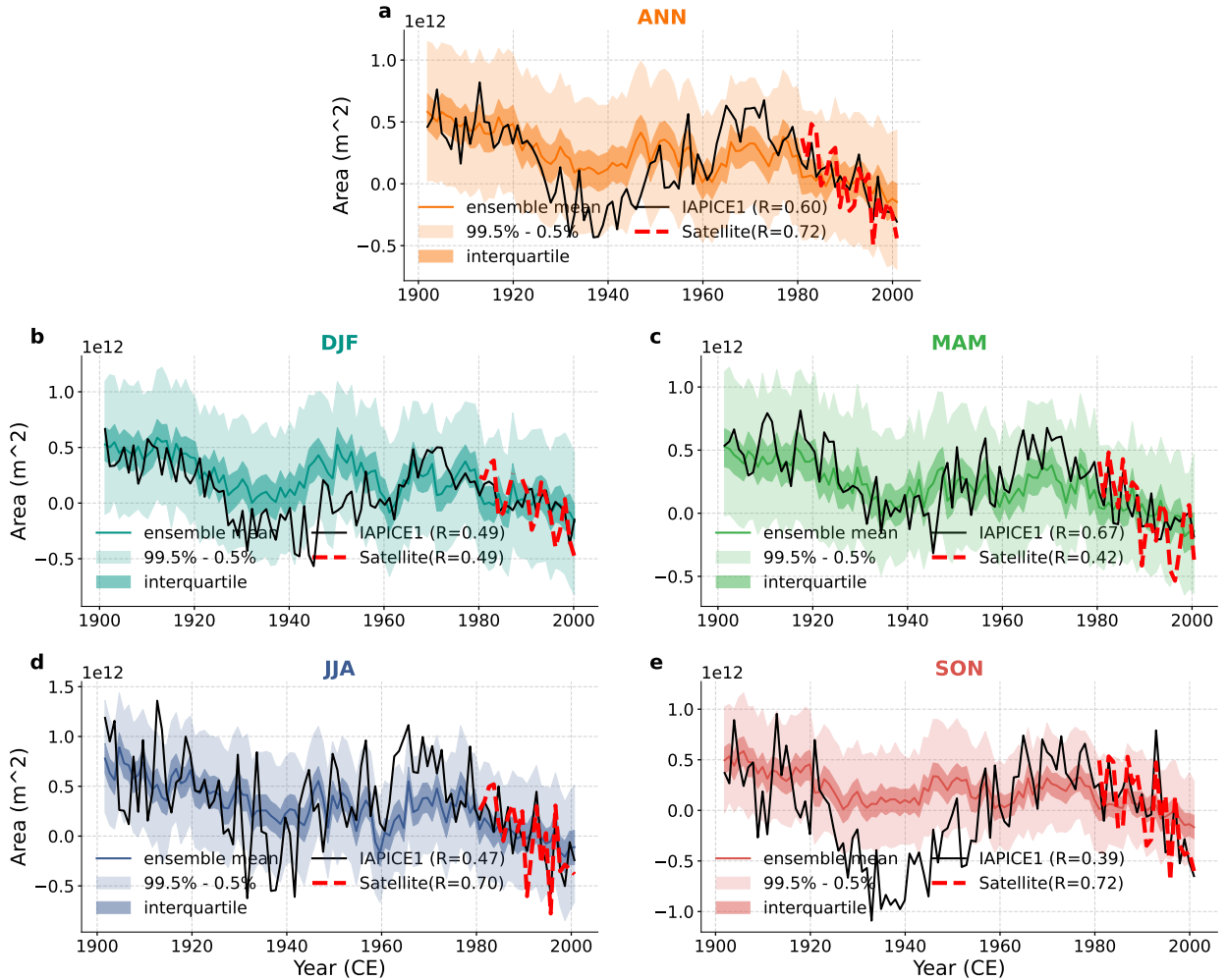


FIG. S10. Same as Fig. S9, but for the period from 1900 to 2000.



18 FIG. S11. Temporal verification of the LMR Seasonal reconstructed NH sea-ice area series (colored curves)
 19 against IAPICE1 (Semenov et al. 2024) sea-ice area (black solid curve) and satellite sea-ice area (Fetterer et al.
 20 2017) (red dashed curve) in annual mean (a), DJF (b), MAM (c), JJA (d), and SON (e). The reference time
 21 period for anomalies is 1980–2000. For each reconstruction, dark shading denotes the ensemble interquartile
 22 range, and light shading the 0.5% to 99.5% interval.

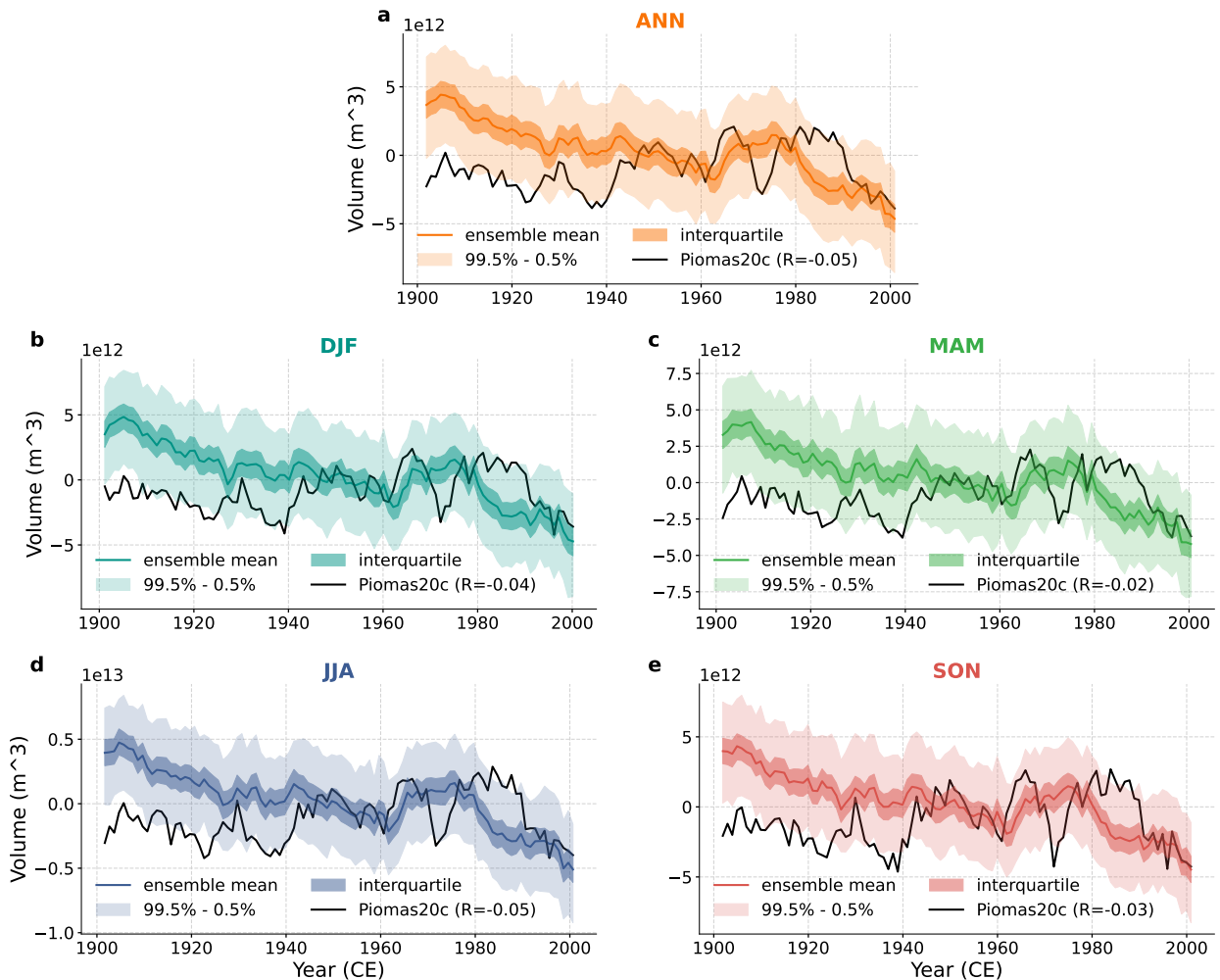
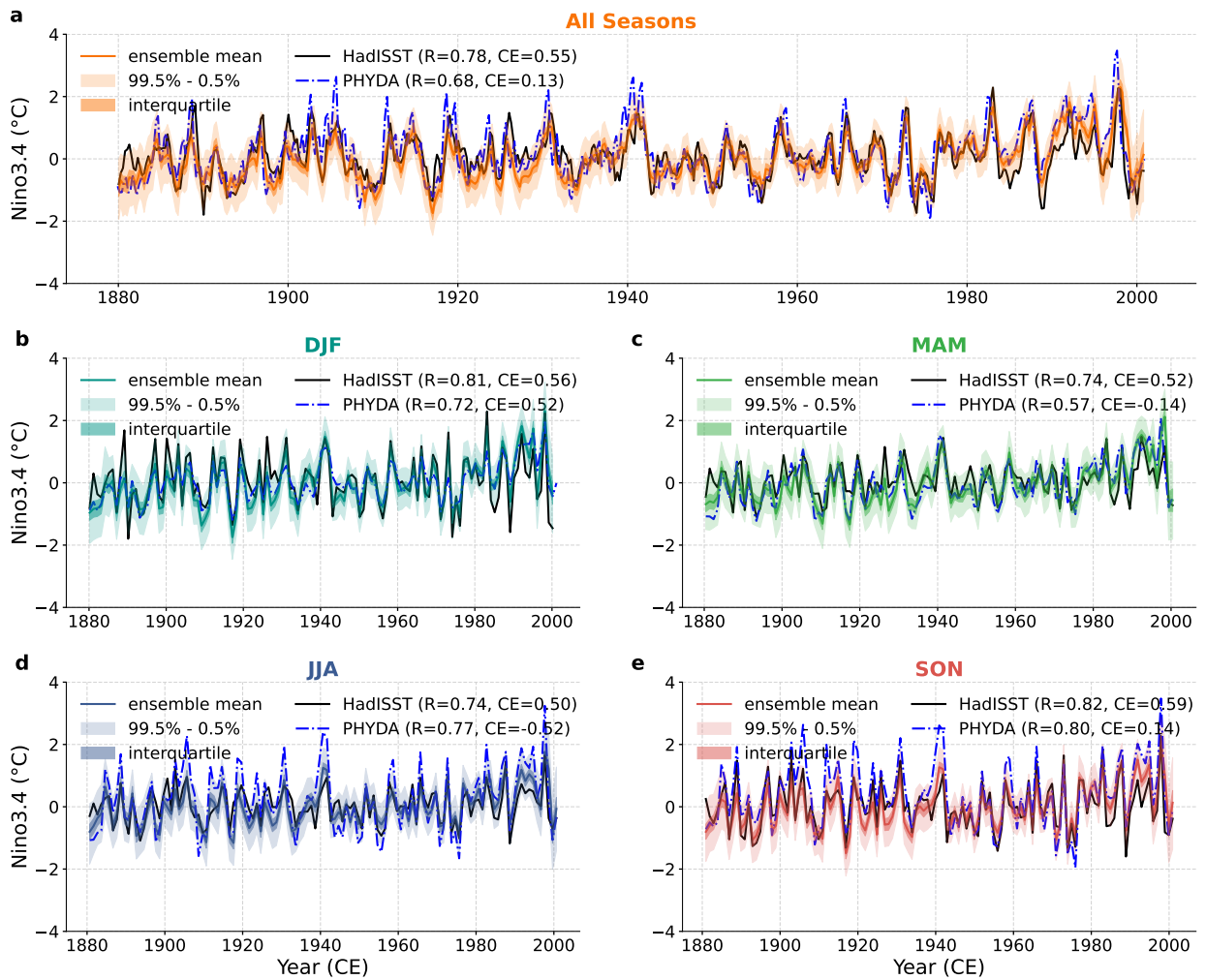


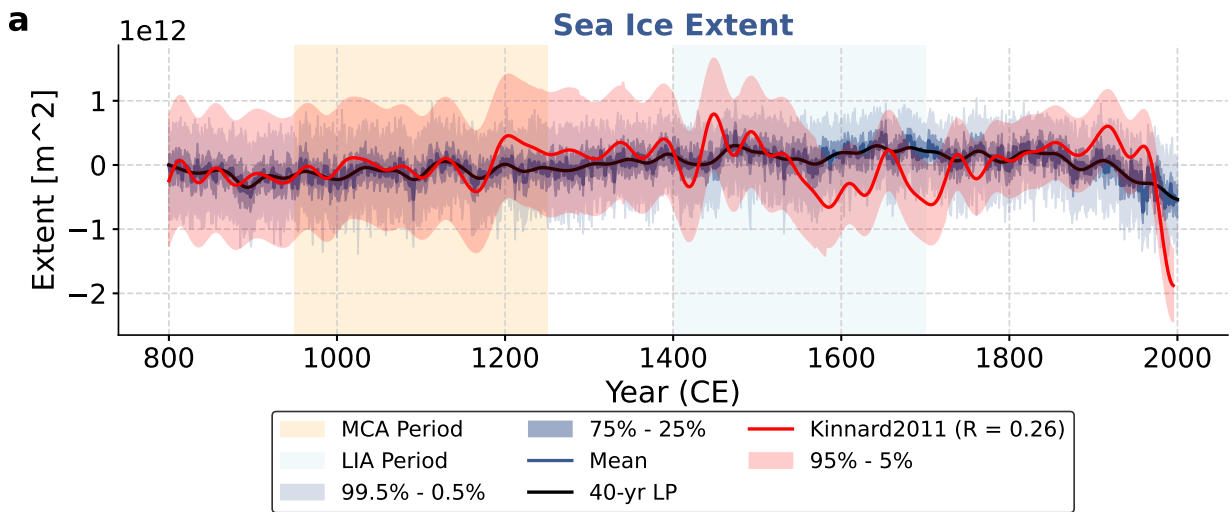
FIG. S12. Same as Fig. 7, but for the NH sea-ice volume.



23 FIG. S13. Same as Figure 8, but with the addition of the PHYDA-reconstructed Niño3.4 Index for comparison.

24 The “R” and“CE” following HadISST (PHYDA) refer to the results comparing HadISST with LMR Seasonal

25 (HadISST with PHYDA).



26 FIG. S14. Sea-ice extent over the last millennium. The LMR Seasonal reconstructed Northern Hemisphere
 27 sea-ice extent (SIE) time series (colored curves) is compared with the 40-year low-pass filtered SIE reconstruction
 28 from [Kinnard et al. \(2011\)](#) (red curve). For LMR Seasonal, the dark blue shading indicates the interquartile
 29 range, and the light blue shading shows the 0.5% to 99.5% confidence interval. The black curve represents
 30 the 40-year low-pass filtered LMR Seasonal mean. Red shading shows [Kinnard et al. \(2011\)](#) the 5% to 95%
 31 confidence interval. R = correlation coefficient between the two 40-year low-pass filtered reconstructions.

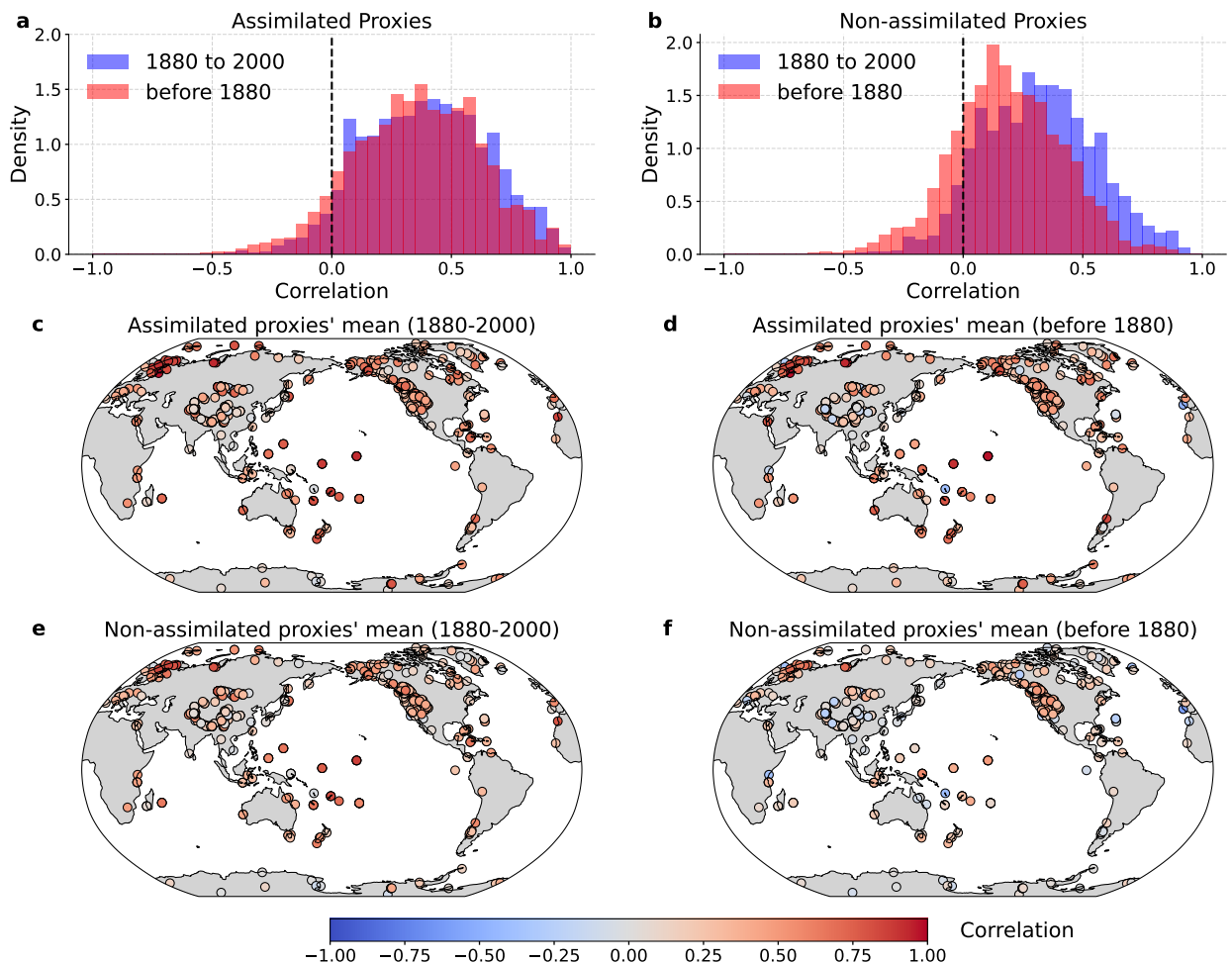


FIG. S15. Same as Figure 12, but for the expert-seasonality based PSM.

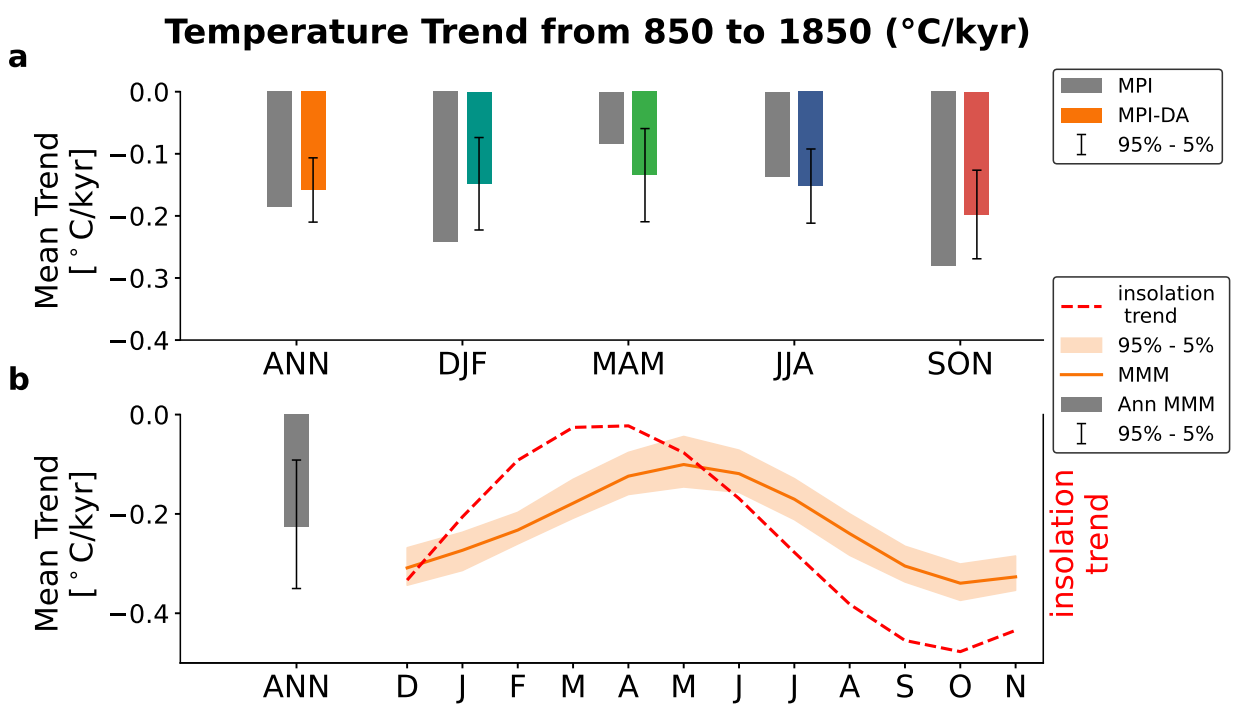


FIG. S16. Same as Figure 13, but for the MPI-ESM-R based DA results and last millennium simulations.

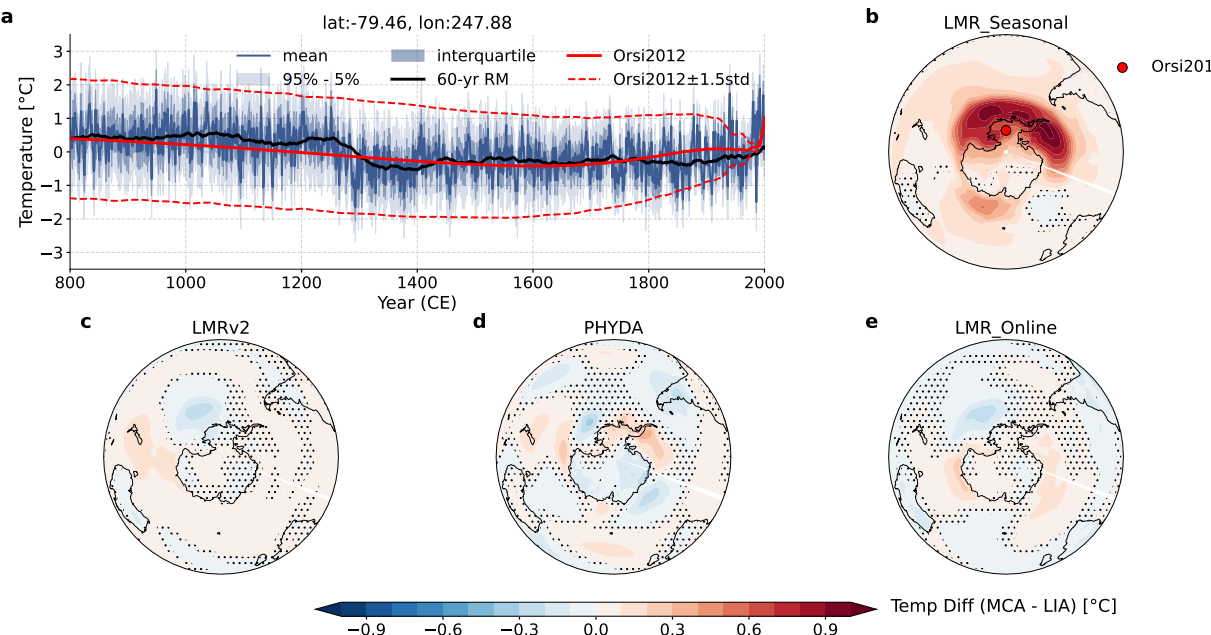
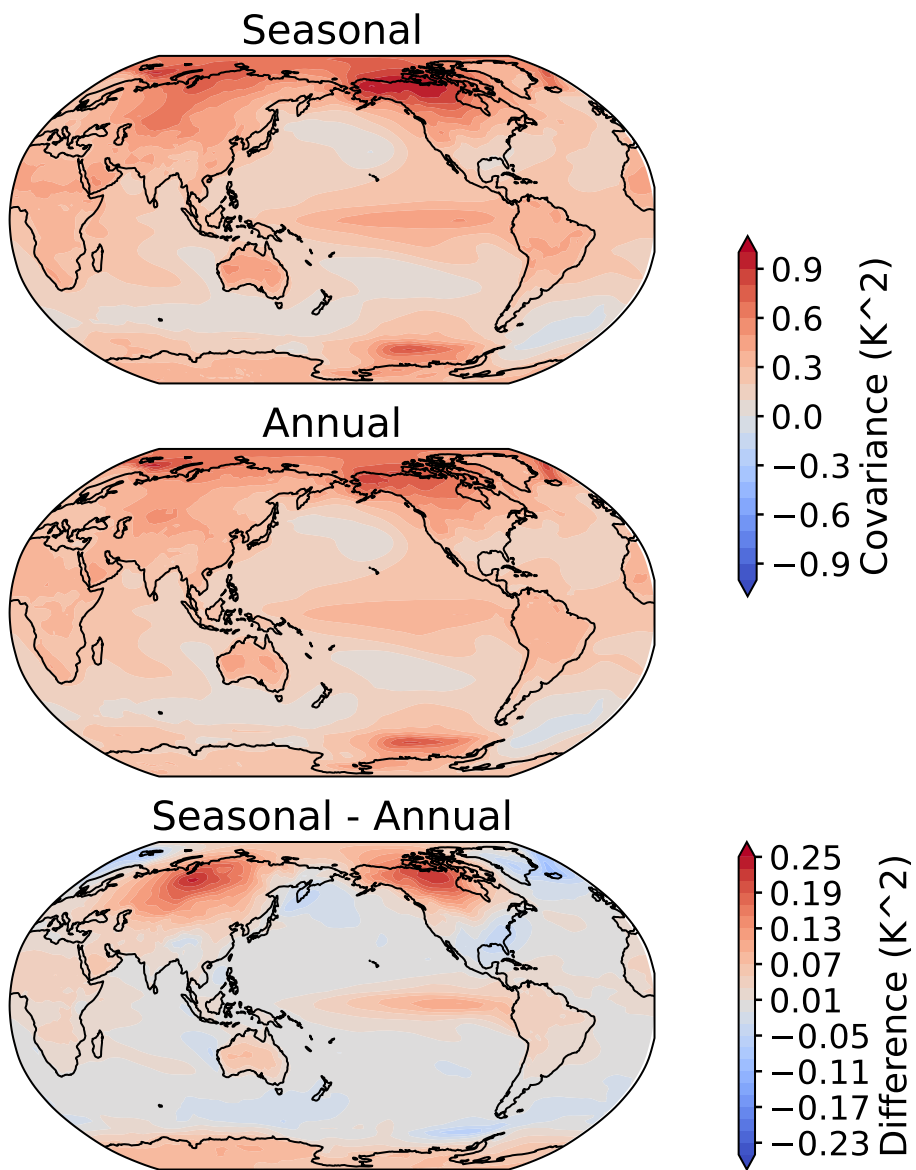


FIG. S17. Time Series of Temperature in West Antarctica (Latitude: -79.46° , Longitude: 247.88°) and MCA-LIA Temperature Difference Patterns in four PDA products. (a) The solid blue colored lines represent the ensemble mean, black solid lines denote the 60-year running means, blue dark shading the interquartile ranges, and light shading the central 95% confidence intervals. The solid red line denotes the temperature reconstruction from the borehole in [Orsi et al. \(2012\)](#), while the dashed red line indicates the 1.5 standard deviation error bar of the borehole reconstruction. (b–e) Southern Hemisphere temperature pattern differences between MCA and LIA from LMR Seasonal (b), LMRv2 (c), PHYDA (d), and LMR Online (e). Black dots denotes regions that do not pass the 95% confidence level according to Student's t-test. The red dot in (b) marks the location of the borehole.



⁴¹ FIG. S18. The covariance between global Mean Temperature and local temperature in seasonal time resolution
⁴² (upper) and annual time resolution (middle) and their difference (lower) in the CCSM4 last millennium simulation.

⁴³ **Appendix: Derivation of the Linear Inverse Model**

⁴⁴ *Derivation of the Linear Inverse Model (LIM) Operator \mathbf{L}*

⁴⁵ The derivation begins from the fundamental equation of the LIM and relates it to the statistical
⁴⁶ properties (covariance matrices) of the system. We begin with the stochastic differential equation
⁴⁷ governing the state vector anomalies $\mathbf{x}(t)$:

$$\frac{d\mathbf{x}}{dt} = \mathbf{L}\mathbf{x} + \boldsymbol{\xi} \quad (1)$$

⁴⁸ where \mathbf{L} is the linear dynamics operator to be determined, and $\boldsymbol{\xi}$ is stochastic forcing, typically
⁴⁹ assumed to be Gaussian white noise with:

$$\langle \boldsymbol{\xi}(t) \rangle = \mathbf{0}, \quad \langle \boldsymbol{\xi}(t)\boldsymbol{\xi}(t')^T \rangle = \mathbf{Q}\delta(t-t'), \quad (2)$$

⁵⁰ where $\langle \rangle$ means expectation.

⁵¹ First, consider the system without noise ($\boldsymbol{\xi} = \mathbf{0}$). Then Eq. (1) becomes:

$$\frac{d\mathbf{x}}{dt} = \mathbf{L}\mathbf{x} \quad (3)$$

⁵² The solution is:

$$\mathbf{x}(t) = e^{\mathbf{L}t}\mathbf{x}(0)$$

⁵³ Define the propagator matrix:

$$\mathbf{G}(t) = e^{\mathbf{L}t} \quad (4)$$

⁵⁴ So the solution becomes:

$$\mathbf{x}(t) = \mathbf{G}(t)\mathbf{x}(0)$$

⁵⁵ Now consider the full system governed by Eq. (1). The solution from time t to $t+\tau$ can be
⁵⁶ expressed as (e.g., [Oksendal 2013](#)):

$$\mathbf{x}(t+\tau) = \mathbf{G}(\tau)\mathbf{x}(t) + \int_t^{t+\tau} \mathbf{G}(t+\tau-s)\boldsymbol{\xi}(s) ds \quad (5)$$

⁵⁷ Define the following covariances under the stationarity assumption:

$$\mathbf{C}(0) = \langle \mathbf{x}(t)\mathbf{x}(t)^T \rangle \quad (6)$$

$$\mathbf{C}(\tau) = \langle \mathbf{x}(t+\tau)\mathbf{x}(t)^T \rangle \quad (7)$$

⁵⁸ Multiply Eq. (5) by $\mathbf{x}(t)^T$ and take the expectation:

$$\begin{aligned} \mathbf{C}(\tau) &= \mathbf{G}(\tau)\langle \mathbf{x}(t)\mathbf{x}(t)^T \rangle + \int_t^{t+\tau} \mathbf{G}(t+\tau-s)\langle \xi(s)\mathbf{x}(t)^T \rangle ds \\ &= \mathbf{G}(\tau)\mathbf{C}(0) + \int_t^{t+\tau} \mathbf{G}(t+\tau-s)\langle \xi(s)\mathbf{x}(t)^T \rangle ds \end{aligned} \quad (8)$$

⁵⁹ Using the property of white noise (Eq. (2)), we know:

$$\langle \xi(s)\mathbf{x}(t)^T \rangle = \mathbf{0}, \quad \text{for } s \geq t \quad (9)$$

⁶⁰ Thus, the integral in Eq. (8) vanishes:

$$\mathbf{C}(\tau) = \mathbf{G}(\tau)\mathbf{C}(0)$$

⁶¹ Solve for the propagator:

$$\mathbf{G}(\tau) = \mathbf{C}(\tau)\mathbf{C}(0)^{-1}$$

⁶² From Eq. (4), we also have:

$$e^{\mathbf{L}\tau} = \mathbf{C}(\tau)\mathbf{C}(0)^{-1} \quad (10)$$

⁶³ Taking the matrix logarithm on both sides of Eq. (10):

$$\begin{aligned} \ln(e^{\mathbf{L}\tau}) &= \ln(\mathbf{C}(\tau)\mathbf{C}(0)^{-1}) \\ \mathbf{L}\tau &= \ln(\mathbf{C}(\tau)\mathbf{C}(0)^{-1}) \end{aligned}$$

⁶⁴ Finally, solve for \mathbf{L} :

$$\mathbf{L} = \tau^{-1} \ln(\mathbf{C}(\tau)\mathbf{C}(0)^{-1})$$

(11)

65 This is the desired expression for the LIM operator \mathbf{L} . It shows how the linear dynamics can be
 66 estimated from the zero-lag and lagged covariance matrices of the observed system at lag τ .

67 *Derivation of the Noise Covariance Matrix \mathbf{Q}*

68 The noise covariance matrix \mathbf{Q} characterizes the stochastic forcing $\xi(t)$ in the LIM equation. Its
 69 derivation relies on the assumption that the system is statistically stationary, meaning the zero-lag
 70 covariance $\mathbf{C}(0)$ is constant in time. We use equations defined in the previous section, such as the
 71 LIM equation Eq. (1) and properties of the noise Eq. (2).

72 The zero-lag covariance matrix is given by Eq. (6):

$$\mathbf{C}(0) = \langle \mathbf{x}(t)\mathbf{x}(t)^T \rangle \quad (12)$$

73 For a statistically stationary process, $\mathbf{C}(0)$ is constant, so its time derivative is zero:

$$\frac{d\mathbf{C}(0)}{dt} = \mathbf{0} \quad (13)$$

74 Using the product rule for differentiation:

$$\frac{d\mathbf{C}(0)}{dt} = \left\langle \frac{d\mathbf{x}(t)}{dt} \mathbf{x}(t)^T \right\rangle + \left\langle \mathbf{x}(t) \left(\frac{d\mathbf{x}(t)}{dt} \right)^T \right\rangle \quad (14)$$

75 Substitute the LIM equation, Eq. (1), $\frac{d\mathbf{x}}{dt} = \mathbf{L}\mathbf{x} + \xi$:

$$\begin{aligned} \frac{d\mathbf{C}(0)}{dt} &= \left\langle (\mathbf{L}\mathbf{x}(t) + \xi(t))\mathbf{x}(t)^T \right\rangle + \left\langle \mathbf{x}(t)(\mathbf{L}\mathbf{x}(t) + \xi(t))^T \right\rangle \\ &= \left\langle \mathbf{L}\mathbf{x}(t)\mathbf{x}(t)^T \right\rangle + \left\langle \xi(t)\mathbf{x}(t)^T \right\rangle + \left\langle \mathbf{x}(t)\mathbf{x}(t)^T \mathbf{L}^T \right\rangle + \left\langle \mathbf{x}(t)\xi(t)^T \right\rangle \\ &= \mathbf{L}\langle \mathbf{x}(t)\mathbf{x}(t)^T \rangle + \langle \mathbf{x}(t)\mathbf{x}(t)^T \rangle \mathbf{L}^T + \langle \xi(t)\mathbf{x}(t)^T \rangle + \langle \mathbf{x}(t)\xi(t)^T \rangle \\ &= \mathbf{LC}(0) + \mathbf{C}(0)\mathbf{L}^T + \langle \xi(t)\mathbf{x}(t)^T \rangle + \langle \mathbf{x}(t)\xi(t)^T \rangle \end{aligned} \quad (15)$$

⁷⁶ To evaluate the noise-state correlation terms, we express $\mathbf{x}(t)$ as the solution to the LIM equation,
⁷⁷ assuming the process started at $t_0 \rightarrow -\infty$:

$$\mathbf{x}(t) = \int_{-\infty}^t e^{\mathbf{L}(t-s)} \boldsymbol{\xi}(s) ds$$

⁷⁸ Then, the first correlation term is:

$$\begin{aligned} \langle \boldsymbol{\xi}(t) \mathbf{x}(t)^T \rangle &= \left\langle \boldsymbol{\xi}(t) \left(\int_{-\infty}^t e^{\mathbf{L}(t-s)} \boldsymbol{\xi}(s) ds \right)^T \right\rangle \\ &= \left\langle \boldsymbol{\xi}(t) \int_{-\infty}^t \boldsymbol{\xi}(s)^T e^{\mathbf{L}^T(t-s)} ds \right\rangle \\ &= \int_{-\infty}^t \langle \boldsymbol{\xi}(t) \boldsymbol{\xi}(s)^T \rangle e^{\mathbf{L}^T(t-s)} ds \end{aligned}$$

⁷⁹ Using the white noise property $\langle \boldsymbol{\xi}(t) \boldsymbol{\xi}(s)^T \rangle = \mathbf{Q} \delta(t-s)$ from Eq. (2):

$$\langle \boldsymbol{\xi}(t) \mathbf{x}(t)^T \rangle = \int_{-\infty}^t \mathbf{Q} \delta(t-s) e^{\mathbf{L}^T(t-s)} ds$$

⁸⁰ The Dirac delta function $\delta(t-s)$ means the integral picks out the value of the integrand at $s=t$.
⁸¹ When the limit of integration coincides with the location of the delta function, the result is typically
⁸² taken as half the value (this corresponds to the Itô interpretation):

$$\langle \boldsymbol{\xi}(t) \mathbf{x}(t)^T \rangle = \frac{1}{2} \mathbf{Q} e^{\mathbf{L}^T(0)} = \frac{1}{2} \mathbf{Q} \quad (16)$$

⁸³ Similarly, for the other term:

$$\langle \mathbf{x}(t) \boldsymbol{\xi}(t)^T \rangle = \left(\langle \boldsymbol{\xi}(t) \mathbf{x}(t)^T \rangle \right)^T = \left(\frac{1}{2} \mathbf{Q} \right)^T = \frac{1}{2} \mathbf{Q}^T \quad (17)$$

⁸⁴ Since \mathbf{Q} is a covariance matrix, it is symmetric ($\mathbf{Q} = \mathbf{Q}^T$). Therefore, the sum of the correlation
⁸⁵ terms is:

$$\langle \boldsymbol{\xi}(t) \mathbf{x}(t)^T \rangle + \langle \mathbf{x}(t) \boldsymbol{\xi}(t)^T \rangle = \frac{1}{2} \mathbf{Q} + \frac{1}{2} \mathbf{Q} = \mathbf{Q} \quad (18)$$

86 Alternatively, this result (**Q**) is standard from the derivation of the Fokker-Planck equation or the
87 covariance evolution equation for linear stochastic systems, where **Q** represents the rate of change
88 of covariance due to noise.

89 Substituting Eq. (18) into Eq. (15) and using the stationarity condition Eq. (13):

$$\mathbf{0} = \mathbf{LC}(0) + \mathbf{C}(0)\mathbf{L}^T + \mathbf{Q} \quad (19)$$

90 This is the continuous-time algebraic Lyapunov equation for a stationary system. It expresses the
91 fluctuation-dissipation theorem for this system: the dissipation of variance by the deterministic
92 dynamics (terms involving **L**) is balanced by the generation of variance by the stochastic forcing
93 (term **Q**).

94 Solving for **Q**:

$$\boxed{\mathbf{Q} = -\left(\mathbf{LC}(0) + \mathbf{C}(0)\mathbf{L}^T\right)} \quad (20)$$

95 This equation allows the estimation of the noise covariance matrix **Q** once the linear operator **L**
96 (from Eq. (11)) and the zero-lag covariance **C**(0) (from data) are known. For **Q** to be physically
97 meaningful as a covariance matrix, it must be positive semi-definite.

⁹⁸ **References**

- ⁹⁹ Fetterer, F., K. Knowles, W. Meier, M. Savoie, and A. Windnagel, 2017: Sea Ice Index, Version 3
¹⁰⁰ [Data Set]. Boulder, Colorado USA. National Snow and Ice Data Center.
- ¹⁰¹ Kinnard, C., C. M. Zdanowicz, D. A. Fisher, E. Isaksson, A. de Vernal, and L. G. Thompson,
¹⁰² 2011: Reconstructed Changes in Arctic Sea Ice over the Past 1,450 Years. *Nature*, **479** (7374),
¹⁰³ 509–512.
- ¹⁰⁴ Oksendal, B., 2013: *Stochastic Differential Equations: An Introduction with Applications*. Springer
¹⁰⁵ Science & Business Media.
- ¹⁰⁶ Orsi, A. J., B. D. Cornuelle, and J. P. Severinghaus, 2012: Little Ice Age cold interval in West
¹⁰⁷ Antarctica: evidence from borehole temperature at the West Antarctic Ice Sheet (WAIS) divide.
¹⁰⁸ *Geophysical Research Letters*, **39** (9).
- ¹⁰⁹ Semenov, V. A., T. A. Aldonina, F. Li, N. S. Keenlyside, and L. Wang, 2024: Arctic Sea Ice Vari-
¹¹⁰ tions in the First Half of the 20th Century: A New Reconstruction Based on Hydrometeorological
¹¹¹ Data. *Advances in Atmospheric Sciences*, **41** (8), 1483–1495.
- ¹¹² Valler, V., and Coauthors, 2024: ModE-RA: a global monthly paleo-reanalysis of the modern era
¹¹³ 1421 to 2008. *Scientific data*, **11** (1), 36.